Additional file 1

Systematic characterization of seed overlap microRNA cotargeting associated with lupus pathogenesis

Hiroki Kitai, Noritoshi Kato*, Koichi Ogami, Shintaro Komatsu, Yu Watanabe, Seiko Yoshino, Eri Koshi, Shoma Tsubota, Yoshio Funahashi, Takahiro Maeda, Kazuhiro Furuhashi, Takuji Ishimoto, Tomoki Kosugi, Shoichi Maruyama, Kenji Kadomatsu, Hiroshi I. Suzuki*

*Corresponding author. Email: hisuzuki@med.nagoya-u.ac.jp (H.I.S.); n-kato@med.nagoya-u.ac.jp (N.K.)

Additional file 1

Figure S1-10

Figure S1

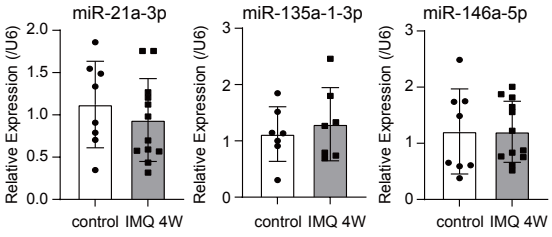

Figure S1. Additional results of qRT-PCR analysis.
Additional validation of downregulated miRNAs by qRT-PCR. Data are means ± SD (N = 8-12).

Figure S2

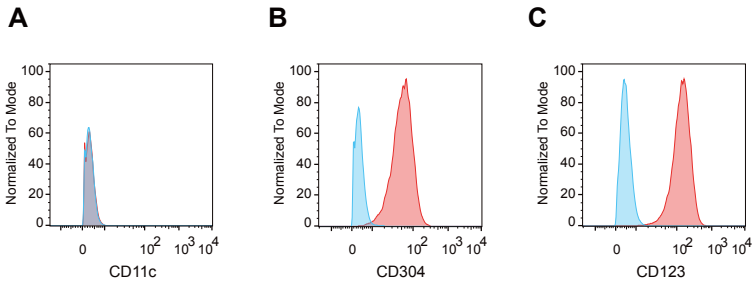

Figure S2. Characterization of the human pDC-like cell line CAL-1.

(A-C) FACS analysis of the cell-surface markers CD11c (A), CD304 (B), and CD123 (C) in CAL-1 cells. Isotype controls are shown in blue.

Figure S3

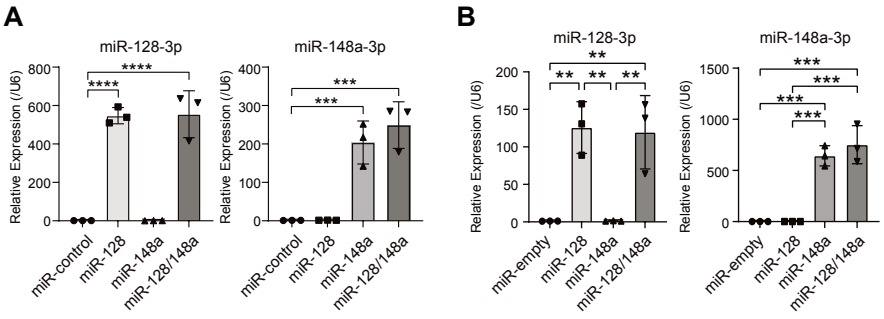

Figure S3. Overexpression of miR-128 and miR-148a in CAL-1 and HeLa cells.

(A) Overexpression of miR-128-3p and miR-148a-3p in CAL-1 cells. Transfection with miR-control, miR-128-3p and miR-control, miR-148a-3p and miR-control, or miR-128-3p and miR-148a-3p, followed by qRT-PCR analysis (N = 3 per group, ***P < 0.001, ****P < 0.0001, one-way ANOVA and post hoc Tukey test).

(B) Overexpression of miR-128-3p and miR-148a-3p in HeLa cells. HeLa cells were transfected with pri-miRNA empty or overexpression plasmids. At 48 hours after transfection, qRT-PCR analyses were performed (N = 3 per group, **P < 0.01, ***P < 0.001, one-way ANOVA and post hoc Tukey test).

Figure S4

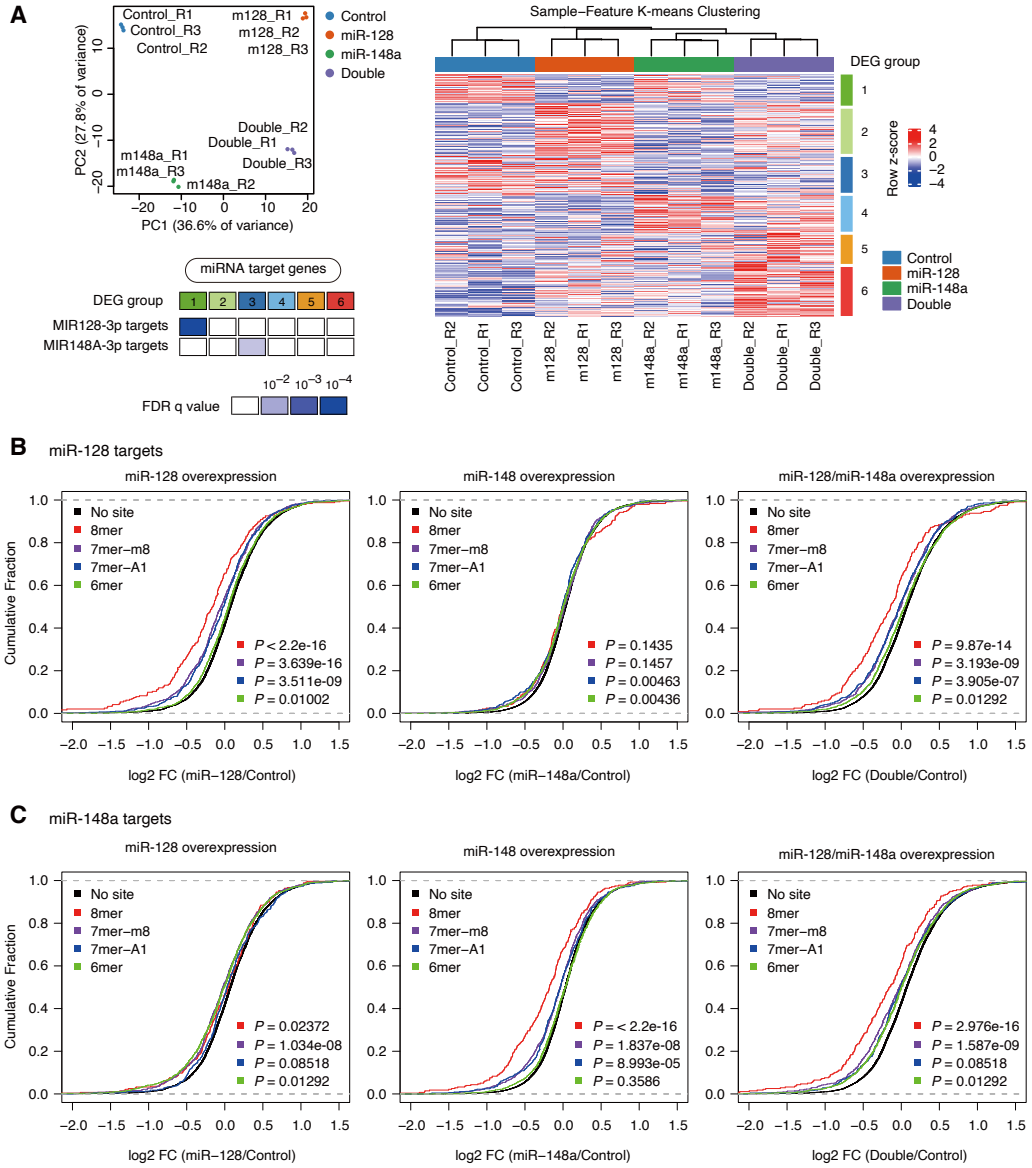

Figure S4. Transcriptomic effects of miR-128 and miR-148a overexpression in HeLa cells.

(A) Principal component analysis (left) and K-means clustering analysis (right) of the 1,000 most variable genes in RNA-seq datasets. The bottom panel shows enrichment of miR-128-3p and mIR-148a-3p target genes in each DEG group, classified by K-means clustering analysis.

(B, C) Cumulative distributions of fold changes (FCs) of genes with single 8mer, 7mer-m8, 7mer-A1, and 6mer sites of miR-128-3p (B) and miR-148a-3p (C) upon single or double miRNA transfection. P values for downregulation (vs. genes with no sites) were calculated by one-tailed Wilcoxon rank sum test.

Figure S5

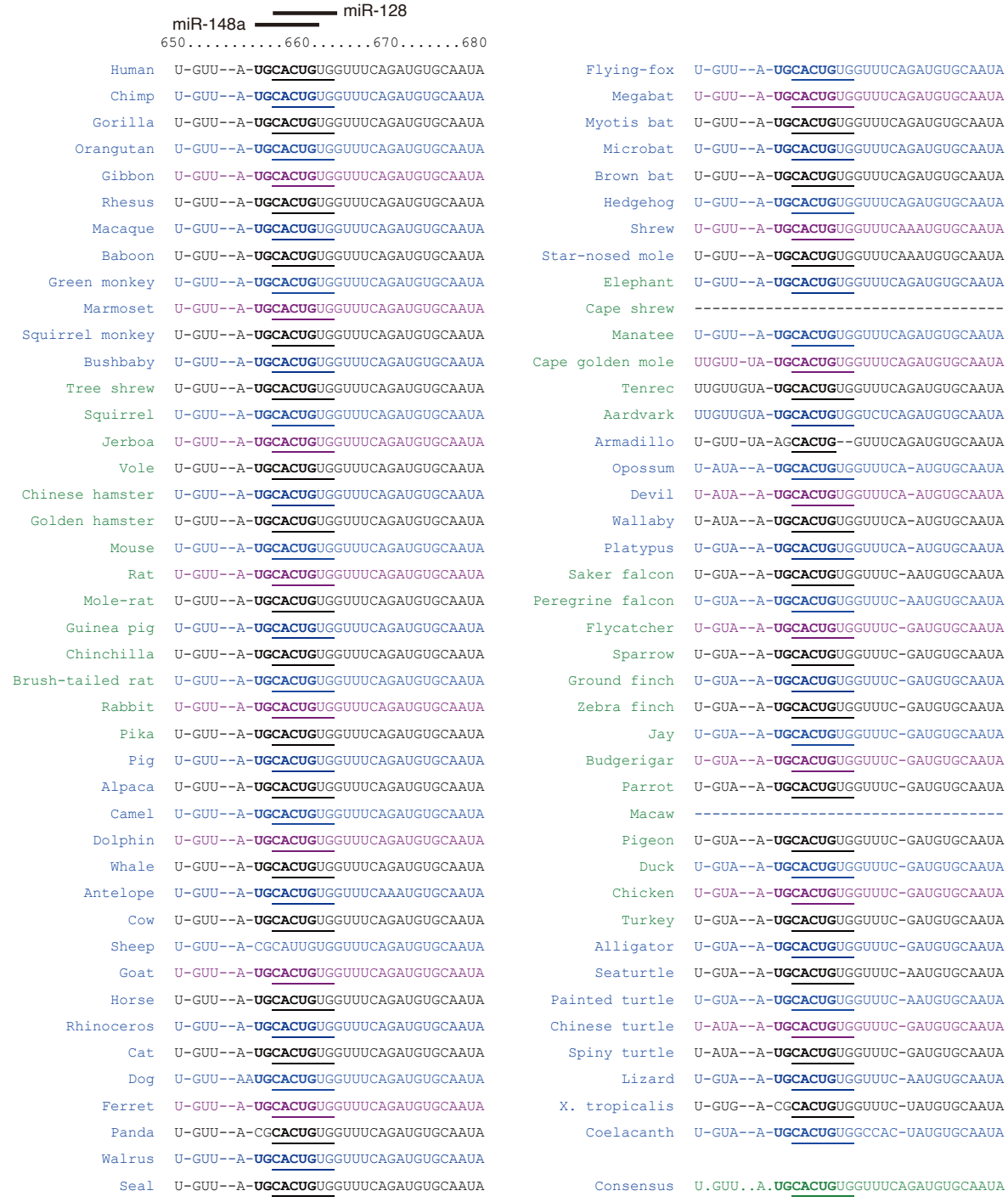

Figure S5. Deep conservation of *KLF4* seed overlap cotarget sites between human and *Coelacanth*. TargetScan sequence alignments around the seed overlap cotarget site within *KLF4* 3′ UTRs are shown.

Figure S6

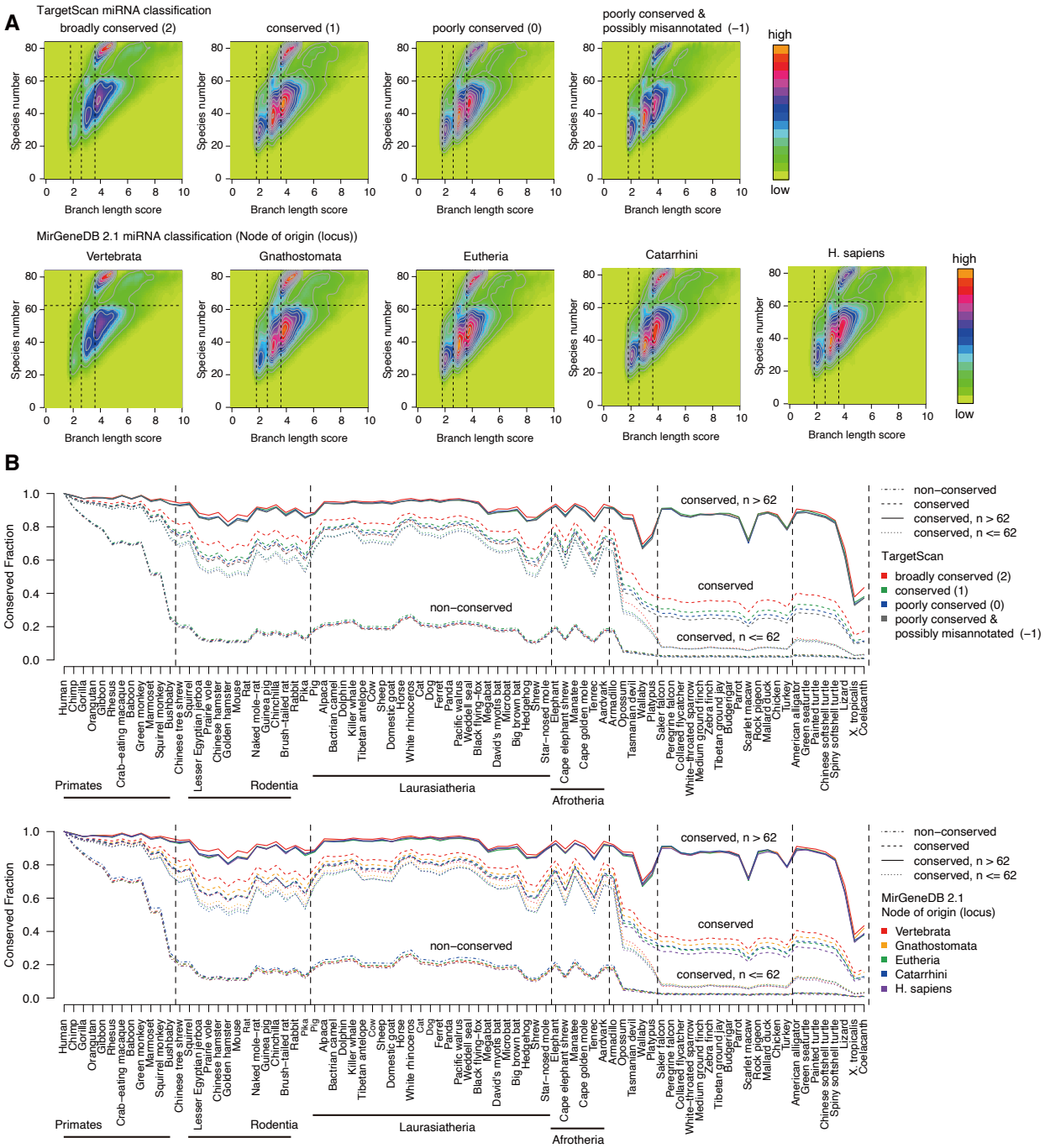

Figure S6. Conservation trends of miRNA target sites based on TargetScan and MirGeneDB classification.

(A) Density and contour plots showing the distribution of BLS values and number of species in which the sites are conserved. Results for target sites of major miRNA groups in TargetScan (top) and MirGeneDB (bottom) classification are shown.

(B) Conservation patterns of non-conserved sites, conserved sites, two classes of conserved sites for major miRNA groups in TargetScan (top) and MirGeneDB (bottom) classification across 84 vertebrate species (according to the species number threshold (n = 62)).

Figure S7

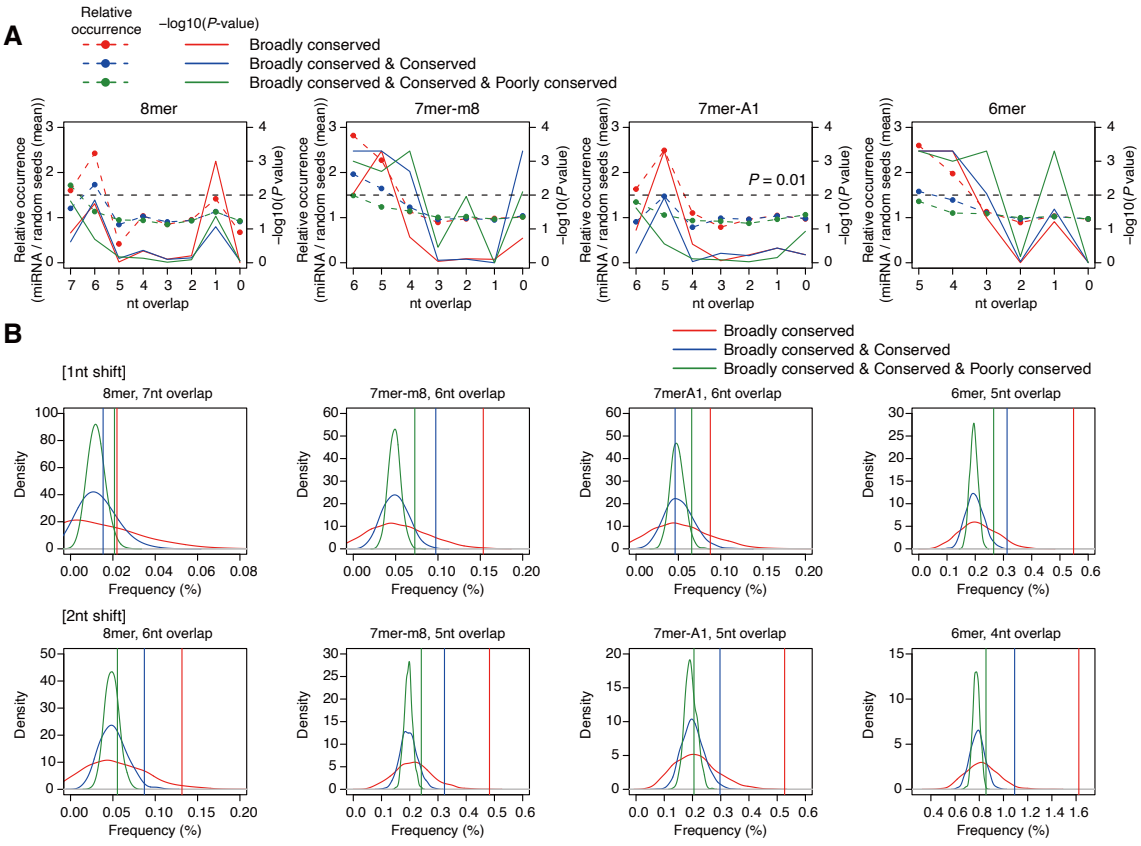

Figure S7. Additional seed overlap analysis of miRNA genes.

(A) Summary showing relative occurrence (dashed lines) and statistics (-log10(*P* value), solid lines) of the maximum overlap for each seed type (8mer, 7mer-m8, 7mer-A1, and 6mer) among all pairs of (1) broadly conserved miRNAs, (2) broadly conserved and conserved miRNAs, and (3) broadly conserved, conserved, and poorly conserved miRNAs. Note that the results were similar when different miRNA groups were combined.

(B) Frequency of extensive seed overlap in real data (vertical lines) and GC content-matched random seed sequences. Results of 1,000 randomizations are shown as density distributions.

Figure S8

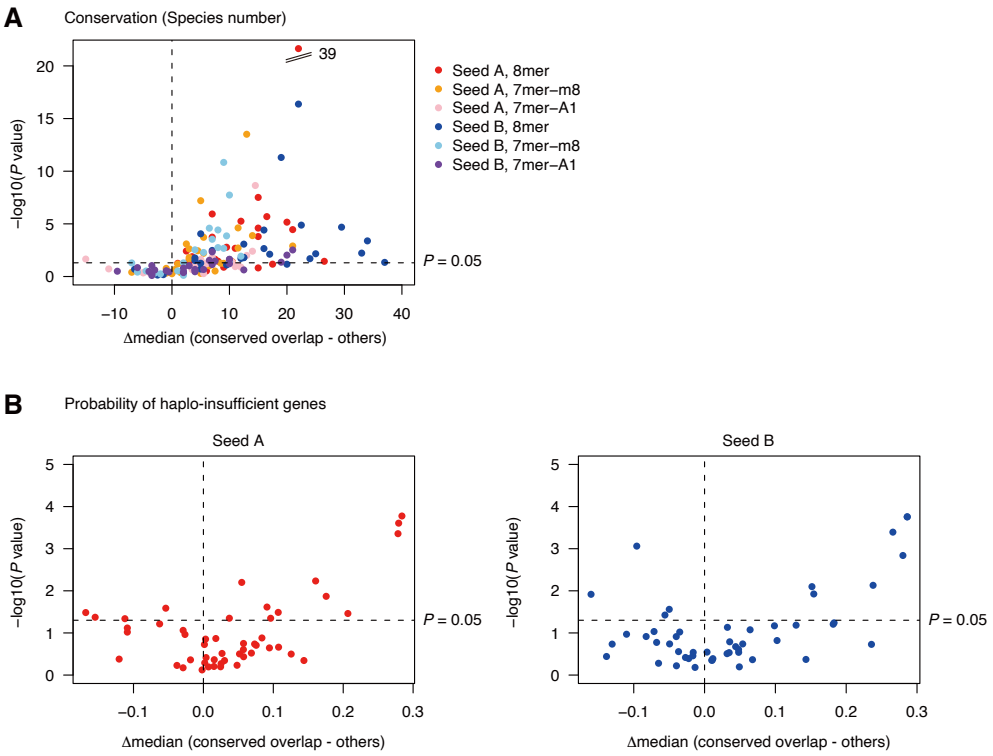

Figure S8. Analysis of evolutionary trends in "seed overlap" miRNA cotargets and probability of haplo-insufficient genes.

(A) Summary of differences and statistics of the number of species in which the sites are conserved. Target sites with "conserved overlap" and other target sites were compared. The results for the 50 miRNA pairs shown in Figure 7 are shown by site type. P values were calculated by one-tailed Wilcoxon rank sum test for either direction.

(B) Summary of differences and statistics of the probability of haplo-insufficient genes between target genes with "conserved overlap" or other target sites. Results for 50 miRNA pairs shown in Figure 7 are shown. P values were calculated by one-tailed Wilcoxon rank sum test for either direction.

Figure S9

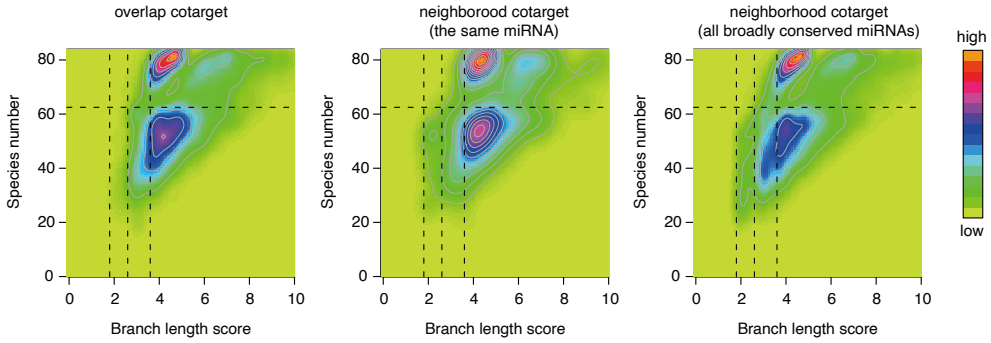

Figure S9. Additional seed overlap analysis of miRNA genes.

Density and contour plots showing the distribution of BLS values and number of species in which the sites are conserved. Results for sites with "seed overlap" cotargeting (left), "neighborhood" cotargeting for the same miRNA (middle), and "neighborhood" cotargeting for all broadly conserved miRNAs (right) are shown. Vertical and horizontal dashed lines indicate BLC cutoffs (1.8 for 8mer, 2.8 for 7mer-m8, and 3.6 for 7mer-A1) and the species number threshold (n = 62). The trends do not markedly differ between groups.

Figure S10

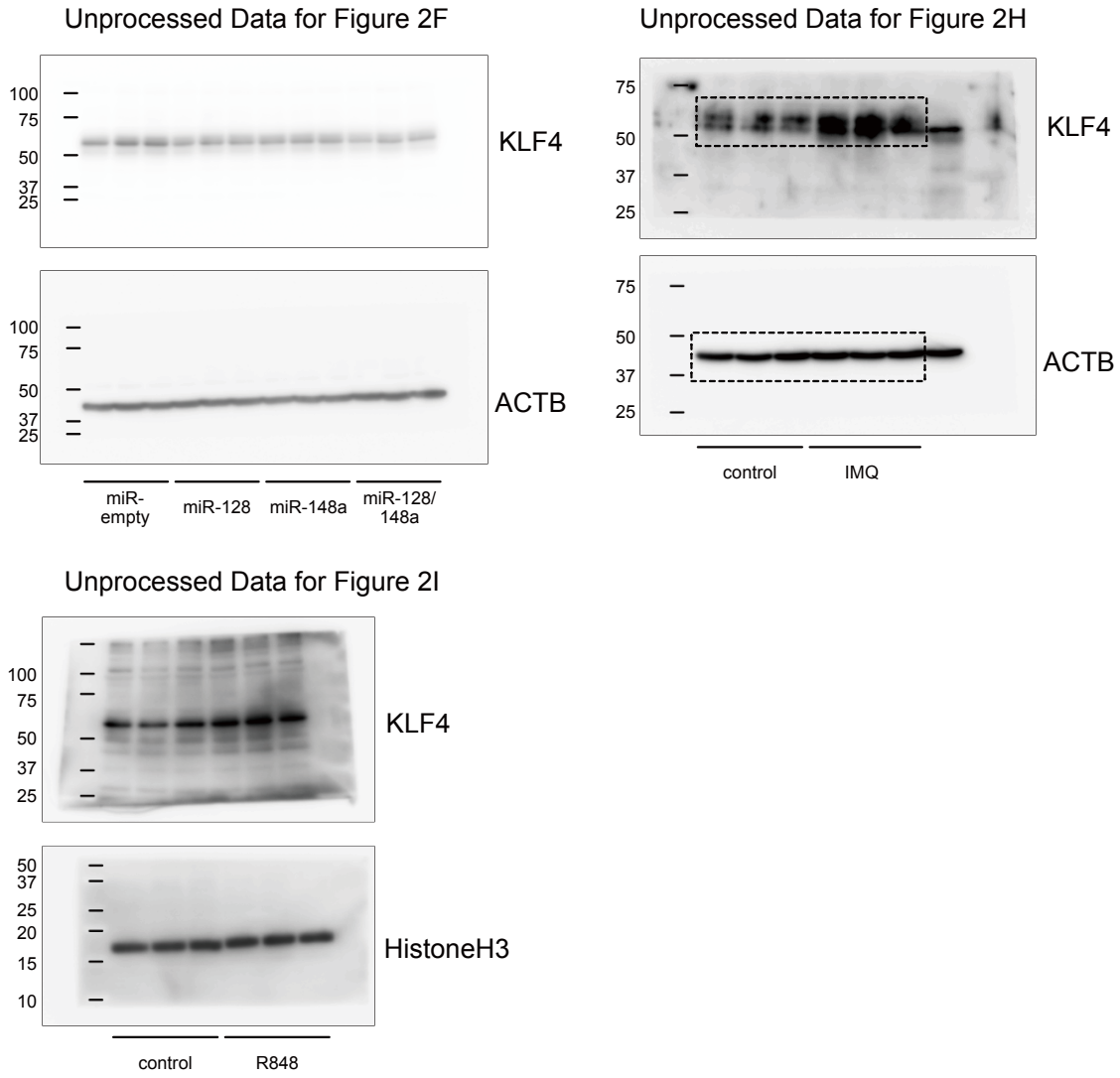

Figure S10. Images of the full-size original blots.
Uncropped images for Fig. 2 are shown.

Additional file 2

Table S1.
The list of up-regulated and down-regulated miRNAs in pDCs from the IMQ mouse model (miRNA microarray analysis).

Table S2.
Summary of the number of seed overlap target sites for 50 miRNA pairs and evolutionary trends, as shown in Figures 7A and 7B.

Table S3.
Summary of the gene set analysis performed using hallmark gene sets (Figure 7D).

Table S4.
Primer information for RT-PCR.

Table S5.
Primer information used for construction of pri-miRNA vectors and KLF4 reporter vector.